(2)

REPORT DOCUMENTATION PAGE

1a. REPORT SECURITY CLASSIFICATION: Unclassified	1b. RESTRICTIVE MARKINGS
2a. SECURITY CLASSIFICATION AUTHORITY	3. DISTRIBUTION/AVAILABILITY OF REPORT: Approved for public release; distribution unlimited.
2b. DECLASSIFICATION/DOWNGRADING SCHEDULE	
4. PERFORMING ORGANIZATION REPORT NUMBER(S)	5. MONITORING ORGANIZATION REPORT NUMBER(S): ARO 24621.3-EG-UIE
6a. NAME OF PERFORMING ORGANIZATION: Massachusetts Institute of Technology, Civil Engineering; 6b. OFFICE SYMBOL (If applicable): CCRE/PACT	7a. NAME OF MONITORING ORGANIZATION: U. S. Army Research Office
6c. ADDRESS (City, State, and ZIP Code): 77 Massachusetts Avenue, Room 1-175, Cambridge, MA 02139	7b. ADDRESS (City, State, and ZIP Code): P. O. Box 12211, Research Triangle Park, NC 27709-2211
8a. NAME OF FUNDING/SPONSORING ORGANIZATION: U. S. Army Research Office; 8b. OFFICE SYMBOL (If applicable):	9. PROCUREMENT INSTRUMENT IDENTIFICATION NUMBER: DAAL03-86-G-0197
8c. ADDRESS (City, State, and ZIP Code): P. O. Box 12211, Research Triangle Park, NC 27709-2211	10. SOURCE OF FUNDING NUMBERS: PROGRAM ELEMENT NO; PROJECT NO; TASK NO; WORK UNIT ACCESSION NO

DTIC ELECTE MAY 01 1989 S E D

11. TITLE (Include Security Classification): Assessment of In-Situ Conditions Using Wave Propagation Techniques

12. PERSONAL AUTHOR(S): Maser, Kenneth; Halabe, Udaya

13a. TYPE OF REPORT	13b. TIME COVERED	14. DATE OF REPORT (Year, Month, Day)	15. PAGE COUNT
Technical	FROM 1/87 TO 12/87	March 1988	42

16. SUPPLEMENTARY NOTATION: The view, opinions and/or findings contained in this report are those of the author(s) and should not be construed as an official Department of the Army position, policy, or decision, unless so designated by other documentation.

17. COSATI CODES		
FIELD	GROUP	SUB-GROUP

18. SUBJECT TERMS (Continue on reverse if necessary and identify by block number): Non-Destructive Testing; Wave propagation sensor techniques; Infrastructure assessment and management; wave form synthesis techniques

19. ABSTRACT (Continue on reverse if necessary and identify by block number)

The overall objective of this research is to stimulate the development of wave propagation sensor techniques for the evaluation of in-situ conditions. Assessment of conditions in the built environment is critical to the management of infrastructure, and there are significant opportunities for developing such sensor technology which have yet to be fully exploited. This research has been directed towards providing a developmental framework, and an associated set of

20. DISTRIBUTION/AVAILABILITY OF ABSTRACT: ☐ UNCLASSIFIED/UNLIMITED ☐ SAME AS RPT. ☐ DTIC USERS	21. ABSTRACT SECURITY CLASSIFICATION: Unclassified
22a. NAME OF RESPONSIBLE INDIVIDUAL	22b. TELEPHONE (Include Area Code) / 22c. OFFICE SYMBOL

developmental tools, applicable to wave propagation techniques. Such techniques include seismics, sonics and ultrasonics, and impulse radar. The research has focused on the development of tools in two areas: (1) predictive analytic models and waveform synthesis techniques, and (2) laboratory evaluation techniques. The development of these tools has been specifically oriented towards applications involving identification, location, and characterization of regular and irregular subsurface anomalies.

Originally this research was conceived in an effort to exploit commonalities between electromagnetic and mechanical wave propagation techniques. As will be discussed in the summary of findings, this perspective was found to be too broad at this stage of the research. Such a perspective will be more meaningful when a better understanding of specific properties of the media is achieved.

ARO 24621.3-EG-UIE

ASSESSMENT OF IN-SITU CONDITIONS USING WAVE PROPAGATION TECHNIQUES

Final Technical Report

by

Kenneth Maser (Principal Investigator)
Udaya Halabe (Graduate Research Assistant)

Period: January 15, 1987 - December 25, 1987

US ARMY RESEARCH OFFICE

Contract/Grant Number
DAAL0386G0197

Massachusetts Institute of Technology

Table of Contents

List of Figures

1 INTRODUCTION

The overall objective of this research is to stimulate the development of wave propagation sensor techniques for the evaluation of in-situ conditions. Assessment of conditions in the built environment is critical to the management of infrastructure, and there are significant opportunities for developing such sensor technology which have yet to be fully exploited. This research has been directed towards providing a developmental framework, and an associated set of developmental tools, applicable to wave propagation techniques. Such techniques include seismics, sonics and ultrasonics, and impulse radar. The research has focused on the development of tools in two areas: (1) predictive analytic models and waveform synthesis techniques, and (2) laboratory evaluation techniques. The development of these tools has been specifically oriented towards applications involving identification, location, and characterization of regular and irregular subsurface anomalies.

Originally this research was conceived in an effort to exploit commonalities between electromagnetic and mechanical wave propagation techniques. As will be discussed in the summary of findings, this perspective was found to be too broad at this stage of the research. Such a perspective will be more meaningful when a better understanding of specific properties of the media is achieved.

2 SUMMARY OF WORK COMPLETED AND IMPORTANT RESULTS

The first year of this research focused on the following two areas:

(a) Electromagnetic wave propagation in construction materials, and

(b) Seismic wave propagation for subsurface condition assessment.

This work is discussed below.

2.1 Electromagnetic Wave Propagation in Construction Materials

A major portion of this research has been devoted to the understanding of electromagnetic wave propagation in construction materials. The research effort has focused on applications which involve the evaluation of bridge decks and pavements using short pulse ground penetrating radars. These applications were chosen because they are also the focus of other ongoing research at MIT, and hence actual field data are available for study. In addition, these applications incorporate many characteristic features of other types of civil engineering structures, and thus the specific results obtained from this study can be generalized to other related applications.

The research efforts can be broken down into the following areas:

(a) Predictive analytic models

(b) Laboratory experiments

(c) Results of numerical studies.

The following section summarizes the work completed and the results obtained in each of the above areas.

2.1.1 Predictive Analytic Models

Development of predictive analytic models was pursued in order to achieve a better understanding of the physics of the problem and to aid in the interpretation of field data. Available analytic models have been pursued as a means for synthesizing radar waveforms representing variable physical conditions. Parametric studies using such waveform synthesis techniques would serve to highlight important features of radar waveforms related to the problem environment. Knowledge of these features will be useful for interpretation of existing field data

and for proposing new measurement approaches. The waveform synthesis technique will also serve to highlight the limitations of radar, since it can theoretically predict what physical characteristics are and are not observable in the waveform, and under what conditions observation is feasible.

Significant progress has been made in the first year of research in the development of analytic tools for waveform synthesis. A radar waveform synthesis computer program, previously developed under an earlier project, was modified to incorporate the effect of reflection from reinforcing steel (rebars) in a bridge deck. This computer program synthesizes radar waveforms for a multilayered medium like a pavement or a bridge deck as shown in Figure 1. The reflections from various layer interfaces (including multiple reflections) are synthesized in the time domain using a one-period sinusoidal transmit pulse of 1 nanosecond duration. The synthesis produces an output waveform as shown in the figure. It may be noted that the two main material property affecting electromagnetic waves are dielectric permittivity and conductivity of the medium. The presence of reinforcement grid in a bridge deck is a very significant environmental parameter and greatly affects the output radar waveform. These rebars can be treated as regular cylindrical subsurface anomalies with a uniform depth and spacing. The reflection from the rebar grid depends on the height and relative position of the radar antenna with respect to this grid. Reflections from this grid couples with the reflections from other irregular subsurface anomalies (e.g., delaminations, deteriorated concrete) which are to be detected. Thus, incorporating the effect of rebars in this model is an important aspect in this study, and must precede any further study to assess the effect of conditions in the neighboring concrete.

In this model the rebar reflection has been modeled using the following Scattering Attenuation Function (SAF) which has been derived based on geometric optics principles (1).

$$SAF = \sqrt{R/(R+d)} \quad (1)$$

where,

SAF = Scattering Attenuation Function, which is defined as the ratio of reflection from a cylinder to that from an infinite flat metal plate at the same location

R = Radius of the cylinder

d = Distance from antenna to the top of the cylinder.

The above equation considers the antenna to be a point source transmitting spherical waves. Each rebar is treated as an isolated cylindrical interface. The normalization of rebar reflection coefficient has been done with respect to that of a flat metal plate, since metals are perfect reflectors with a reflection coefficient of -1. The above equation has been derived for large diameter scatterers whose diameter exceed one-fifth of a wavelength. The wavelength of 1 GHz electromagnetic pulse (which is characteristic of the antennas used for bridge deck and pavement studies) in normal concrete is about 10 cm, and thus one-fifth of a wavelength amounts to 2 cm. The diameter of No. 6 rebars, which represent the typical size used in concrete bridge decks is about 1.9 cm. Thus, these rebars lie at the lower limit of applicability of geometric optics principles. The validity of this model for this limiting case has been established by laboratory experiments as discussed in the next section. Some existing solutions for reflection from infinitely long cylindrical scatterers incident by plane electromagnetic waves (2) were also investigated but were found to predict much higher value for SAF than observed experimentally. This is probably because the wavefronts emitted by the radar antennas used here are closer to spherical in shape and thus the ray optics theory of Eq. (1) gives better results.

Eq. (1) gives the effect of a single rebar. The total effect is obtained by adding the contribution of the individual bars which fall within the radiation cone of the antenna. This leads to the issue of determining the radiation pattern of the antenna. In addition, the reflection from

rebars also depends on their orientation with respect to the direction of polarization of the antenna. These phenomena are very difficult to model mathematically, and the available solutions in the literature on electromagnetic wave theory consider idealized case of a point source or infinite line source emitting plane or cylindrical wavefronts, respectively (1,2). Since the actual antenna is an extended source with finite dimensions, the characterization becomes even more complex. Thus, an empirical approach has been followed for this case. The above phenomenon have been observed experimentally as described in the next section, and empirical techniques have been used to incorporate the above effects in the modeling of rebars in the waveform synthesis program (see Sections 2.1.2 and 2.1.3).

The next important issue is the modeling of reflections from irregular subsurface anomalies like delaminations and deteriorated concrete. Modeling of electromagnetic properties of concrete needs to be considered to understand the propagation of electromagnetic waves within deteriorated concrete. This issue will be the focus of the second year of this research.

2.1.2 Laboratory Experiments

To verify the applicability of Eq.(1) for the case of rebars, laboratory experiments were conducted using the setup shown in Figure 2. Two types of antenna were used, namely the air-coupled horn-type (ACH)[1] antenna and the ground coupled dipole (GCD)[2] antenna. Both operate at a center frequency of approximately 1 GHz. The ACH antenna is normally used for mobile horizontal surveys with shallow (up to 1 meter) penetration requirements. The GCD antenna is used for detecting buried objects like pipes and rebars. In the case of the ACH

[1] Manufactured by Penetradar, Inc., Niagara Falls, NY, and integrated into a system by Gulf Applied Research, Marietta, GA. This entire radar unit was loaned to MIT by the Federal Highway Administration.

[2] Manufactured by Geophysical Survey Systems, Inc., Hudson, NH.

antenna, the rebar was placed over a styrofoam block which has a relative dielectric permittivity of 1 (same as that for air). For the GCD antenna, the rebar was buried in sand (instead of concrete) to facilitate easy placement and removal. In addition to rebar reflections, waveforms were also recorded from reflections off of a large metallic plate.

Rebars and metallic cylinders of various diameters were used, all placed at the same location for a given antenna. Waveforms were obtained for each diameter cylinder with each antenna. A waveform was also obtained for the setup without any plate or rebar. All waveforms were digitized and stored. This last waveform served as a reference and was subtracted from all the other waveforms (using processing software), thus eliminating the effect of internal antenna reflections. The reflected wave peak amplitudes from the rebars and cylinders were normalized by the reflected wave peak amplitude from the metal plate to obtain the SAF. Results of these experiments vs. the theoretically predicted curve using Eq.(1), for varying sizes of the scattering rebars and metallic cylinders, have been plotted in Figures 3 and 4.

Figure 3 for the ACH antenna shows that the results predicted by Eq.(1) are within 10 to 15% of the experimental value for cylinders with radii ranging from 1 to 3 cm. This corresponds to rebar sizes ranging from #6 to #11. #6 rebars are common transverse reinforcement in bridge decks. Longitudinal reinforcement in bridge decks, and reinforcement in concrete pavement is usually of smaller diameter. Figure 4 for the GCD antenna shows similar results, but with a deviation of 20 to 25% in the 1 to 3 cm radius range. The SAF values are higher here due to the fact that the cylinders are positioned closer to the antenna. It is interesting to note that for both antennas the SAF appears to become insensitive to radius outside of the range discussed above. Confirmation of this would require more detailed experimentation. The specific results obtained

indicate that smaller diameter longitudinal rebar (#4's and #5's) are almost as influential in the radar waveform as large diameter (#6) transverse bars. Examination of field data will help to shed some light on this prediction.

An important thing to note in the modeling of rebars is that the ACH and GCD antennas are linearly polarized. This means that they will tend to show a much stronger response to cylinders oriented parallel to the polarization direction of electric field. To study this effect, a similar experiment to that described above was conducted. In this second experiment, the orientation of the rebar was continuously varied with respect to the direction of electric field polarization of the antenna. Figures 5 and 6 show the experimentally obtained variation in SAF with respect to the polarization direction. The result for the ACH antenna (Figure 5) show that the effect of orientation is more significant at small diameters. This result has been predicted analytically for the case of an infinitely long wire antenna (1). For example, SAF for a #6 bar reduces by 85% in going from parallel to perpendicular to the direction of antenna polarization. The equivalent reduction for a 2.5 cm radius pipe is less than 60%. The results for the GCD antenna show a much stronger reduction in orientation sensitivity with increasing cylinder radius. This is most likely due to the closer proximity of the cylinders to the antenna in this experiment. The cylinders are occupying a larger percentage of the cone of radiation, and the response to the polarized waves is more complex.

The issue of polarization is important in the investigation of reinforced concrete because it indicates the contribution of rebars of different orientation. The results in Figure 5, for example, indicate that in a longitudinal bridge deck survey (with antenna orientation typically longitudinal), the dominant transverse rebar will have a relatively small effect on the radar waveform. This observation suggested that only one set of rebar need to be considered in the waveform synthesis model.

The above study considers the effect of a single isolated rebar placed at a central location with respect to the antenna. In practice, two or more rebar will fall within the radiation pattern of the antenna at different locations from its center. The SAF studied above can be applied to each rebar to yield the response of multiple rebars. However, consideration must also be given to the radiation pattern of the antenna and its effect on the amount of energy arriving at each rebar. The radiation pattern supplied by manufacturers prescribe the energy emitted along a sphere or a cylinder (i.e., constant distance from the source), not along a plane, such as that represented by a rebar grid. Thus, experiments were conducted to obtain radiation pattern in a plane. This pattern is a characteristic of the type of antenna used. Since most field data of interest to this study have been collected using the ACH antenna, the radiation pattern was constructed for this antenna alone. The pattern was determined by conducting an experiment similar to the one as described earlier, this time using a signal diameter rebar and moving it in a horizontal plane. The rebar orientation was kept parallel to the polarization direction of the electric field (which is the prominent orientation). The pattern of reflected wave amplitude for a No. 6 rebar is shown in Figure 7. The amplitudes corresponding to various rebar positions have been normalized by the reflection from the central position of the rebar, which is the position producing the maximum effect. Such normalized plots have been found to be almost the same for different diameter of rebars or metallic cylinders. Figure 7 shows that amplitude reduces to half of its maximum value when the rebar is at a distance of about 14 inches from the central position. For the height of the antenna (above the rebar) of 17 inches, this corresponds to an angle of about 40 degrees on either side of the central vertical axis of the antenna.

This result has been adapted for use in the waveform synthesis model by considering the following simplification. In the model it has been assumed that the antenna has a cone of radiation ($\pm 40°$) into which a certain number of rebars will fall. The intensity of the radiation

pattern has been assumed to be uniform within this cone (given by Eq.1 for each rebar), and all rebars falling outside this cone have been ignored. This approximation is consistent with the current level of sophistication in the model.

Another important issue for waveform synthesis is to determine the exact nature of the transmit pulse emitted by the particular antenna. For this purpose, the same experimental setup shown in Figure 2 was used. Following the procedure described earlier (to obtain SAF), the shape of the reflected pulse from a metal plate was recorded. This has been shown in Figure 8 for the ACH antenna. Since metal plate is a perfect reflector with a reflection coefficient of -1, this shape is just an inverted transmit pulse. It can be seen from Figure 8 that the transmit pulse is very nearly sinusoidal with the negative peak to positive peak time span (i.e., half of time period) of 0.5 nanosecond. Thus, it has been concluded that the transmit pulse can be approximated by a sinusoidal pulse with a time period of one nanosecond. The idealized transmit pulse used in the synthesis program is shown in Figure 9. This pulse is a one-cycle sinusoid with tapered ends to reflect the continuity of the actual pulse. The amplitude of this pulse has been taken arbitrarily as unity, with no loss of generality .

2.1.3 Results of Numerical Studies

The findings described in the two previous sections have been incorporated in the waveform synthesis program mentioned earlier. The synthesis program at present models a bridge deck or pavement as a multilayered medium with homogeneous layers as was shown in Figure 1. Each of these layers is characterized by a thickness (t), an electrical conductivity (σ), a relative dielectric permittivity (ε) and a relative magnetic susceptibility (μ). μ is usually unity for dielectric materials used in construction. For a given set of physical parameters, the program computes the reflection and transmission coefficients at each interface, and the time of travel and

attenuation of electromagnetic pulse within each layer. The radar antenna is assumed to be a point source with the receiver coincident with the transmitter. The capability of computing reflection from rebar grids has been implemented using the equations and empirical procedure described in the previous two sections. The program takes into account the effect of various multiple reflections between the layer interfaces. Using the transmit pulse shown in Figure 9, the program synthesizes waveforms corresponding to given sets of input parameters (layer and rebar geometry, and layer properties). A typical waveform generated by this computer program is shown in Figure 10. Reflections from various interfaces have been shown in this figure.

The above synthesis program has been used to conduct a parametric study representing bridge deck deterioration conditions. The parameters were determined to represent normal variations as well as deterioration conditions. To illustrate the latter, it has been found that the top concrete cover disintegrates into a cohesionless "soil", apparently due to freeze/thaw cycles. This mechanism creates expansion which increases the porosity of the concrete. The porosity increase can lead to a higher or lower than normal moisture content, depending on the moisture environment. Both porosity and moisture content have a strong effect on dielectric permittivity of concrete.

The dielectric permittivity of concrete can approximately be obtained using the following three-phase mixture formula (3).

$$\sqrt{\varepsilon_r} = (1-\phi)\sqrt{\varepsilon_m} + S\phi\sqrt{\varepsilon_w} + (1-S)\phi\sqrt{\varepsilon_a} \ldots \quad (2)$$

where,

ϕ = porosity of concrete

S = degree of saturation

ε_m = relative dielectric permittivity of concrete solids (~~6)

ε_w = relative dielectric permittivity of water (= 81)

ε_a = relative dielectric permittivity of air (= 1)

ε_r = relative dielectric permittivity of resulting concrete mixture

The above equation was used to assess the range of dielectric permittivity values associated with various conditions which could be encountered in the field. For a porosity of 10%, the dielectric permittivity of concrete varies from 6.3 to 9.6 for degree of saturation varying from 25% to 100%. This corresponds to a moisture content of 1% of 4.2%. For a higher value of porosity of 15%, the dielectric permittivity of concrete ranges from 6.4 to 11.8, corresponding to a range of degree of saturation from 25% to 100%. In this case, the corresponding range of moisture content is 1.7% to 6.7%. The upper and lower values of these ranges are associated with the possible occurrence of freeze-thaw damage.

Table 1 summarizes the physical properties considered in the parametric study. Note that the values for asphalt and concrete conductivity in the bridge decks are taken to be much higher than reported laboratory values, due to the presence of high amounts of chlorides and moisture. Reported conductivities for asphalt and concrete are 1.25 and 5.00 mmho/meter, respectively (5). For the purpose of this parametric study, these values have been increased by a factor of 10.

Table 1: Material Properties Used for Parametric Study

Properties	Normal Concrete	Low-Moisture Deteriorated Concrete	High-Moisture Deteriorated Concrete
ε (asphalt)	5.0	5.0	5.0
σ (asphalt), mmho/m	12.5	12.5	12.5
ε (cover concrete)	9.0	7.0	12.0
σ (cover concrete), mmho/m	50.0	50.0	200.0
ε (lower concrete)	9.0	9.0	9.0
σ (lower concrete), mmho/m	50.0	50.0	50.0

Note: ε = dielectric permittivity

σ = conductivity

This parametric study assumed a bridge deck with a total concrete thickness of 8 inches overlain by asphalt. The thickness of asphalt was varied from between 1.5 and 3.5 inches, representing typical conditions encountered in the field. The cover concrete thickness (portion of concrete above the top rebar grid) was varied between 1.0 inch and 3.0 inches. This variation has been observed in the field. Low values of cover have been correlated with corrosion-induced delamination. Rebars consisting of No. 6 rebar at 6 inches spacing top and bottom were considered in this study. The bottom rebars were assigned constant effective cover (measured from the bottom) of 1.5 inches. Three different field conditions were considered, with the corresponding layer properties, as given in Table 1.

Samples of the synthesized waveforms generated in the parameter study are shown in Figures 11 and 12. Since the properties of asphalt have been taken as constant in all these cases, amplitude of the first reflection from the asphalt surface remains the same. However, the amplitude of reflection from subsequent interfaces shows a considerable change. Figure 11 shows the influence of moisture content. Carter et al (4) observed such changes in radar field waveforms and suggested an empirical parameter (called R_2) as a possible indication of deterioration of cover concrete. This measure, R_2 is defined as the ratio of reflected amplitude from the asphalt-concrete interface to that from top asphalt surface (C/A from Figure 10). Values of R_2 for some of the cases considered in this parametric study have been shown in Figure 13. The proposed ratio appears to be constant for a given moisture content at sufficiently large asphalt and cover concrete thicknesses. However, the magnitude of R_2 changes dramatically for small values of asphalt and concrete cover thickness, as can be seen from Figure 13. This is because of the overlap of reflections from the two consecutive interfaces when the interfaces are close. The influence of such a change in geometry on the waveform pattern can be seen in Figure 12. Another empirical measure (called R_4) has been proposed in this study. This ratio has been defined as the ratio of reflected amplitude from top rebar grid to that from the asphalt-concrete interface (D/C from Figure 10). Values of R_4 for some typical cases considered in this parametric study have been shown in Figures 14 and 15. It can be seen that this ratio is not affected by change in asphalt thickness but still breaks down for low cover concrete thickness. Also, these figures show that R_4 is more sensitive to changes in cover concrete condition than R_2, and could provide a more sensitive measure.

A number of concrete bridge decks in the New England area have been surveyed using the ACH antenna as a part of another ongoing research project at MIT. Typical field waveforms are shown in Figure 16. Such field data have shown that in some cases the layer interfaces and rebars show prominently, while in other cases, the reflections from consecutive interfaces

overlap, resulting in a more complex pattern. An attempt is presently being made to compute R_2 and R_4 ratios for field data and study how they correlate with actual deterioration observed in the field. Another observation from the field data is that wave attenuation in the field is much higher than predicted by the theoretical model, and in most cases the bottom of the deck is not observable. This suggests that there are loss mechanisms which are not being properly taken into account in the model. The field waveforms also indicate the presence of dispersion; that is, the waveforms tend to spread out as it gets deeper into the concrete. This indicates that the material properties of concrete are frequency dependent. The typical short pulse radar is not a true monochromatic source but emits energy in a wide frequency band. This band is shown in Figure 17 for the ACH antenna. Therefore, it is important to consider the effect of frequency dependence of material properties in waveform synthesis as well as in field interpretation of the data. The above observations suggested future research place a stronger emphasis on characterization and modeling of electromagnetic properties of concrete.

Some attempt is being made to experimentally determine the nature of property variation (e.g., moisture and chloride content) across discontinuities or cracks, and these results can be extrapolated to estimate the dielectric permittivity and conductivity variation on two sides of the crack. It may be mentioned here that air-filled cracks and delaminations are not easily detectable. These cracks may, however, be filled with moisture and chloride, and may be associated with material property contrasts on either side. These latter phenomena are likely to cause an observable impact on the radar waveforms. The characterization and modeling of such discontinuities and delamination will be studied in the second year of this research.

2.2 Seismic Wave Propagation for Subsurface Condition Assessment

A portion of the first year of this research has been devoted to the study of transmission characteristics of seismic boundary waves at the interface between the two dissimilar media. This study was motivated by other MIT research in which seismic boundary waves have been studied as a means for detection of leakage in large liquid containments. The phenomenon of reflection and transmission of seismic waves at an interface is conceptually very similar to that of electromagnetic waves considered earlier. The wave impedance of the medium in the case of electromagnetic wave propagation is a function of conductivity and dielectric permittivity (which affects the wave velocity) of the layer. For seismic waves, wave impedance is a function of wave velocity and material density. The conventional seismic body waves (P- and S-waves) are commonly employed to detect thick subsurface layers and their properties in geophysical exploration. However, these waves are not capable of identifying changes in the small region under a tank or impoundment bottom as would occur in the soil due to leakage. On the other hand, seismic boundary waves (Stoneley waves) that propagate along the interface between two or more dissimilar materials are very sensitive to the conditions at or near the vicinity of the boundary (6). Thus they are highly suitable for early detection of deterioration and leakage at the interface created by a tank or impoundment bottom. Once leakage occurs, the properties of the soil region affected by leakage are altered due to increased fluid content and buoyancy. Thus, an interface is created between the soil region unaffected by leakage and the region which is affected.

In the measurement procedure, described in (6), a seismic source is set off on one side of the containment, and the Stoneley waves propagating along the bottom are received and recorded by a series of receivers placed on the opposite side (Figure 18). The waves passing through the leak-affected region exhibit a time delay and amplitude loss compared to the waves passing

through the unaffected zone, and this forms the basis for leak detection. Part of the amplitude loss due to leakage is due to transmission loss similar to that which would be experienced by a radar wave passing through deteriorated concrete. A wave propagating through a leakage area first crosses the interface between the sound and the leakage area, and then crosses a second interface when it comes out of this leakage region. The total transmission loss is a combination of increased attenuation in the leak-affected zone, and the product of the two transmission coefficients associated with the two crossings noted above. This latter effect had never been studied or documented. To study this effect theoretically, it was necessary to obtain expression for transmission coefficient of Stoneley waves.

No simple expression was found in the literature for reflection and transmission coefficients for Stoneley waves. Some researchers have proposed complex numerical models for reflection and transmission coefficient for Rayleigh waves (7,8,9), which are boundary waves similar to Stoneley waves but which occur at an air-solid interface. These models are mathematically complex and considerable effort would have been required to program them and derive the necessary results. Instead of following this approach, an attempt was made to study the validity of using P- and S-wave transmission coefficients as an approximation. Both Rayleigh and Stoneley waves consist of P- and S-waves. S-waves can be further divided into SH-waves and SV-waves. SH-waves have displacement components that are polarized perpendicular to the plane of incidence. The displacement components of SV-waves are polarized in the plane of incidence (10). For normal incidence the transmission coefficients for P-, SH-, and SV-waves are given by (10):

$$T_{12} = \frac{2\rho_1 c_1}{\rho_1 c_1 + \rho_2 c_2} \tag{3}$$

where,

T_{12} = amplitude transmission coefficient for wave propagating from medium 1 into medium 2

ρ_1 = density of medium 1 (incident medium)

c_1 = corresponding wave velocity in medium 1 (incident medium)

ρ_2 = density of medium 2 (transmitted medium)

c_2 = corresponding wave velocity in medium 2 (transmitted medium)

The suggestion considered here is to estimate Stoneley wave transmission coefficients by substituting Stoneley wave velocities for the two media (sound area and area affected by leakage into C_1 and C_2 of Eq.(3). This suggestion is supported by numerical results obtained for Rayleigh wave transmission from Plexiglas to polystyrene and vice verse (7) as shown in Table 2. The values of Rayleigh wave velocities and densities used in this numerical study are typical of the soil properties characterizing the leak detection. It can be seen from this table that the transmission coefficients predicted using Eq.(3) are very close to the values obtained by Alsop et al. (7) using their complex numerical model, and the product of the two transmission coefficients (which is the required factor as mentioned earlier) obtained from the two approaches differ by less than two percent. Therefore Eq.(3) gives a reasonable estimate for the transmission coefficient for Rayleigh waves and similar results would be expected for Stoneley waves. Also, it is clear from the numerical results that the transmission loss associated with the product of transmission coefficients is fairly small.

Table 2: Transmission Coefficient for Rayleigh Waves for the Data Presented by Alsop et al. (7)

Properties of 1st Medium (Plexiglas)	Properties of 2nd Medium (Polystyrene)	Transmission Coefficients Obtained by Alsop et al. (7)	Transmission Coefficients Obtained Using Eq.(3)
$c_1 = 1280$ m/sec	$c_2 = 1080$ m/sec	$T_{12} = 1.216$	$T_{12} = 1.145$
$\rho_1 = 1.22 t/m^3$	$\rho_2 = 1.08 t/m^3$	$T_{21} = 0.796$	$T_{21} = 0.855$
		$T_{12}\,T_{21} = 0.968$	$T_{12}\,T_{21} = 0.979$

An attempt was made to understand the generation and propagation of Stoneley waves more extensively for the purpose of synthesizing waveforms. Such synthetic waveforms could then be used to theoretically study the effect of small amount of leakage from the tank bottom. A review of the work done by other researchers in this area was conducted. Geophysicists normally use Stoneley wave propagation in a borehole (often called tube waves) to study rock properties. Various researchers have studied the propagation of Stoneley waves in boreholes (11) and the effect of in-situ permeability on such propagation (12). Some researchers have also generated synthetic waveforms for the study of such guided wave propagation in fluid-filled boreholes (13, 14). A review of this literature revealed that waveform synthesis for Stoneley waves would be mathematically complex, and would involve a considerable time and effort. A decision was therefore made to discontinue this work in favor of further work dealing with electromagnetic waves.

3 Discussion and Future Direction

It has become clear from this research effort that wave propagation techniques is too broad a subject to serve as a focus for a single research project. Basic issues regarding electromagnetic and mechanical wave propagation characteristics in construction materials of interest require further understanding. Some of these have been raised in this research, and others undoubtedly exist. Once such an understanding is achieved, then a more unified treatment would be appropriate. From a practical point of view, it appears that electromagnetic wave propagation techniques should be the preferred direction of future research. These techniques are least understood in the civil/construction environment, and offer substantial promise in speed, coverage, and information content.

It has also become clear that predictive analytic models, such as the waveform synthesis described in this report, must build on a more fundamental understanding of the propagation properties in the media. As the research progressed it became clear that many more of the propagation properties needed to be understood, particularly with radar. This realization was stimulated by large quantities of field data generated by another MIT Project (The "Bridge Deck Project"). Some of the radar propagation properties, such as reflections at interfaces and effects of uniform changes in moisture content, can be understood by applying basic solutions in electromagnetic theory. Field conditions such as chloride and moisture infiltration, concrete disintegration, and cracking are not easily quantifiable. Therefore, much of this understanding will have to be achieved by creating and measuring these conditions in the laboratory.

Based on these observations, it is recommended that further research be directed towards understanding the EM wave propagation characteristics of construction materials. Of all materials of potential interest, reinforced concrete is the one which is least understood, and

where radar would be most useful. Therefore, the work should combine theoretical studies in which various material characteristics have been idealized, and laboratory studies where the idealizations and solutions are not available or practically achievable.

4 References

(1) Davis, C.W., III, "A Computational Model for Subsurface Propagation and Scattering for Antennas in the Presence of a Conducting Half Space," Technical Report 479X-7, ElectroScience Laboratory, Department of Electrical Engineering, The Ohio State University, Columbus, Ohio 43212, October 1979.

(2) Kong, J.A., Electromagnetic Wave Theory, John Wiley & Sons, New York, 1986.

(3) Feng, Shechao, and Sen, P.N., "Geometrical Model of Conductive and Dielectric Properties of Partially Saturated Rocks," Journal of Applied Physics, Vol.58, No.8, October, 1985.

(4) Carter, C.R., Chung, T., Holt, F.B. and Manning, D.G., "An Automated Singal Processing System for the Signature Analysis of Radar Waveforms from Bridge Decks," *Canadian Electrical Engineering Journal*, Vol.11, No.3, 1986.

(5) Ulriksen, C.P.F., Applications of Impulse Radar to Civil Engineering, published by Geophysical Survey Systems, Inc., Hudson, NH, 1983.

(6) Maser, K.R. and Kaelin, J.J., "Leakage Detection of Liners Using Seismic Boundary Waves," Proceedings of the 6th National Conference on Management of Uncontrolled Hazardous Waste Sites, 1985.

(7) Alsop, L.E., Goodman, A.S., and Gregersen, S., "Reflection and Transmission of Inhomogeneous Waves with Particular Application to Rayleigh Waves," *Bulletin of the Seismological Society of America*, Vol.64, No.6, December, 1974.

(8) Chen, T.C. and Alsop, L.E., "Reflection and Transmission of Obliquely Incident Rayleigh Waves at a Vertical Discontinuity Between Two Welded Quarter-Spaces," *Bulletin of the Seismological Society of America*, Vol.69, No.5, October 1979.

(9) McGarr, A., and Alsop, L.E., "Transmission and Reflection of Rayleigh Waves at Vertical Boundaries," *Journal of Geophysical Research*, Vol.72, No.8, April, 1967.

(10) Kolsky, H., Stress Waves in Solids, Dover Publications, New York, 1963.

(11) Cheng, C.H. and Toksoz, M.N., "Generation, Propagation and Analysis of Tube Waves in a Borehole, SPWLA Twenty-Third Annual Logging Symposium, July 6-9, 1982.

(12) Cheng, C.H., Zinzhong, Z., and Burns, D.R., "Effects of In-Situ Permeability on the Propagation of Stoneley (Tube) Waves in a Borehole," submitted to *Geophysics* in December, 1985.

(13) Cheng, C.H. and Toksoz, M.N., "Elastic Wave Propagation in a Fluid-Filled Borehole and Synthetic Acoustic Logs," *Geophysics*, Vol.46, No.7, July 1981.

(14) Rosenbaum, J.H., "Synthetic Microseismograms: Logging in Porous Formations," *Geophysics*, Vol.39, No.1, February 1974.

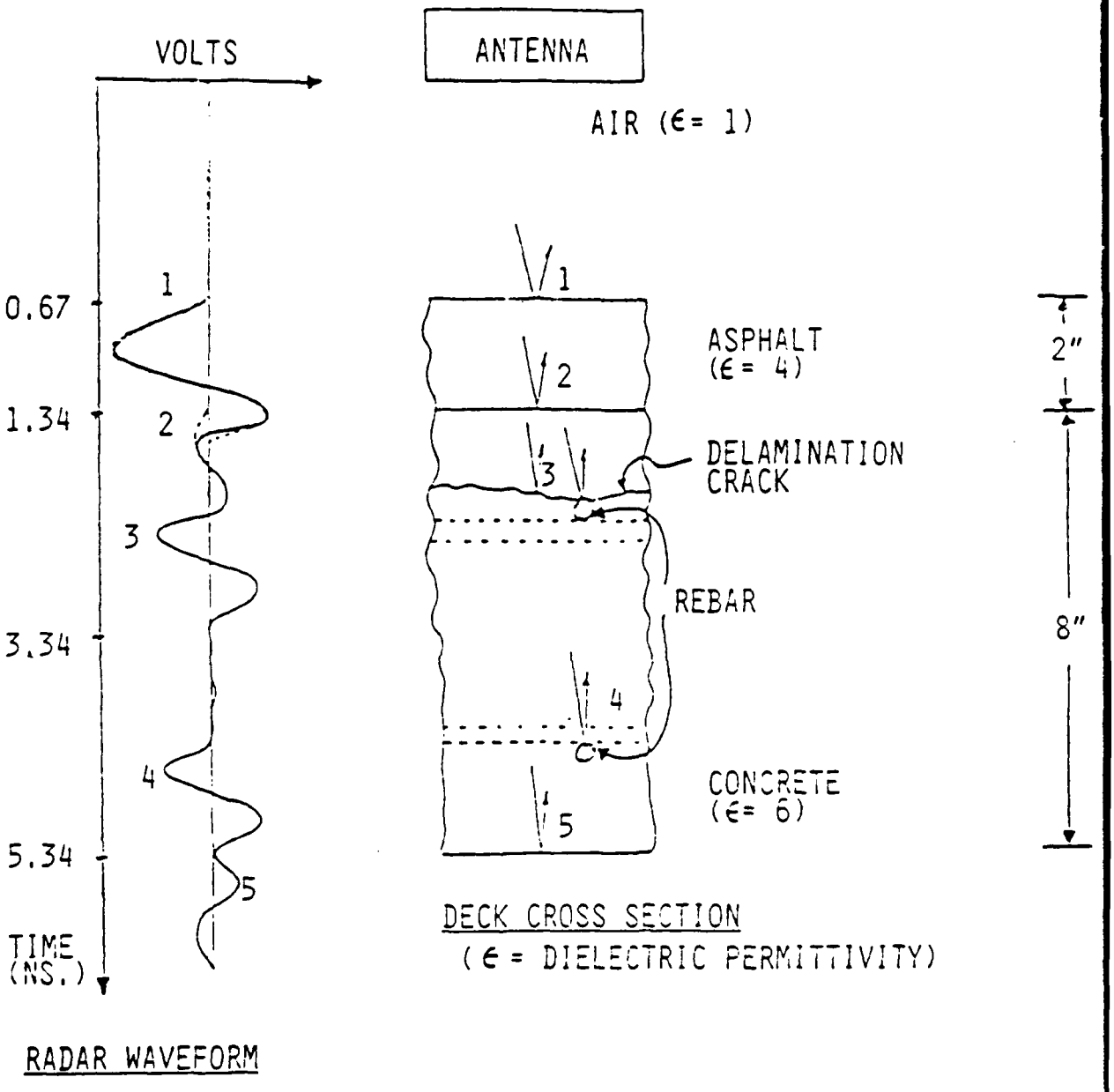

Figure 1

BRIDGE DECK MODEL

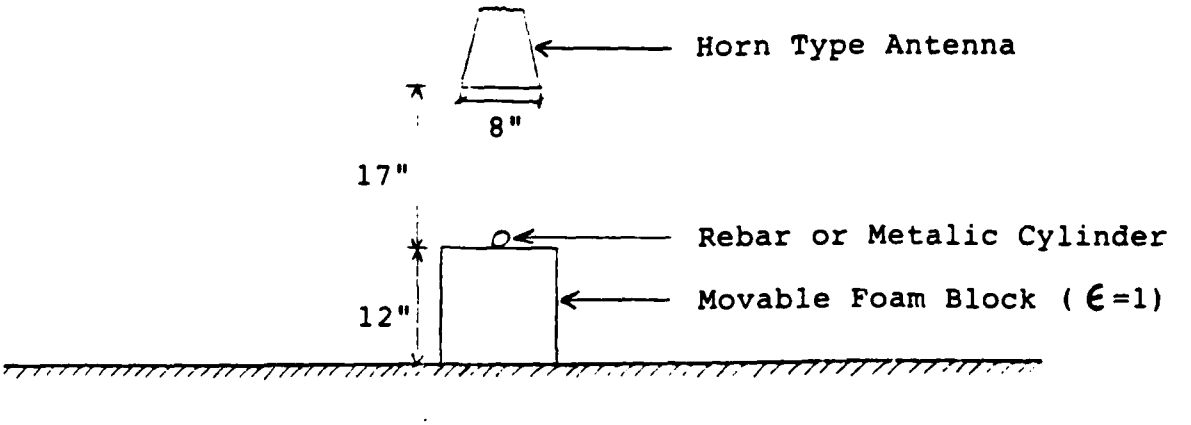

LABORATORY SETUP FOR AIR-COUPLED ANTENNA (ACH)

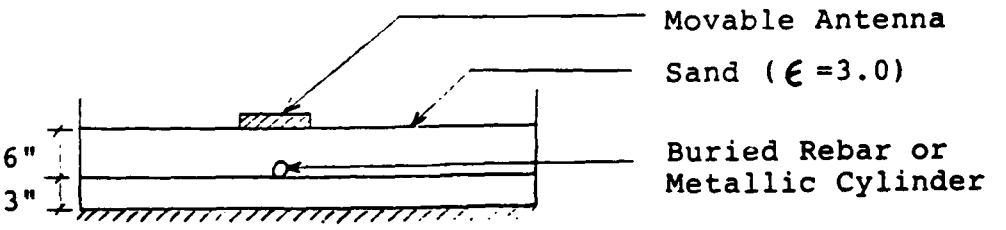

LABORATORY SETUP FOR GROUND-COUPLED ANTENNA (GCD)

Figure 2

LABORATORY SETUP FOR STUDYING REFLECTION FROM
REBARS OR METALLIC CYLINDERS

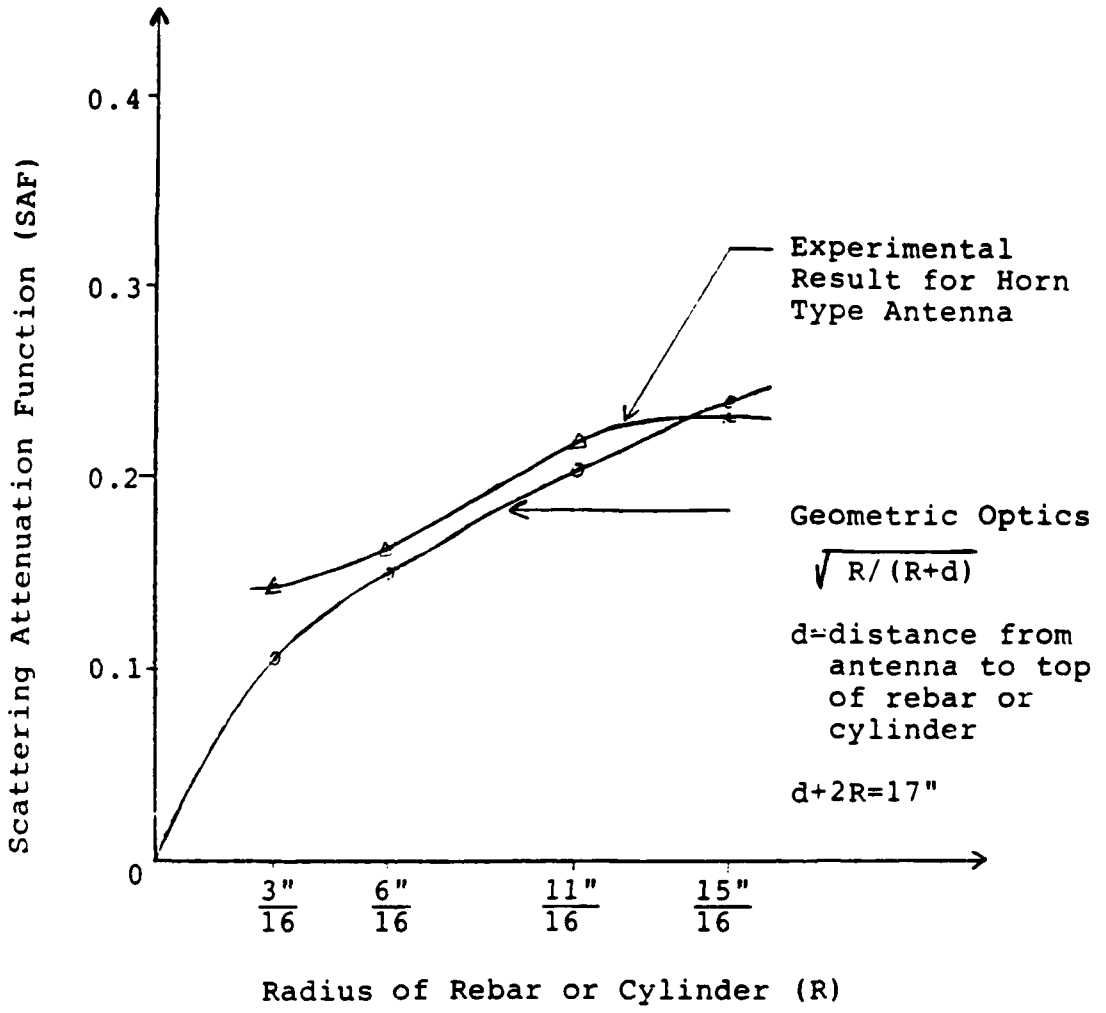

Figure 3

SCATTERING ATTENUATION FUNCTION (SAF) FOR ACH ANTENNA

(Rebar oriented parallel to polarization direction)

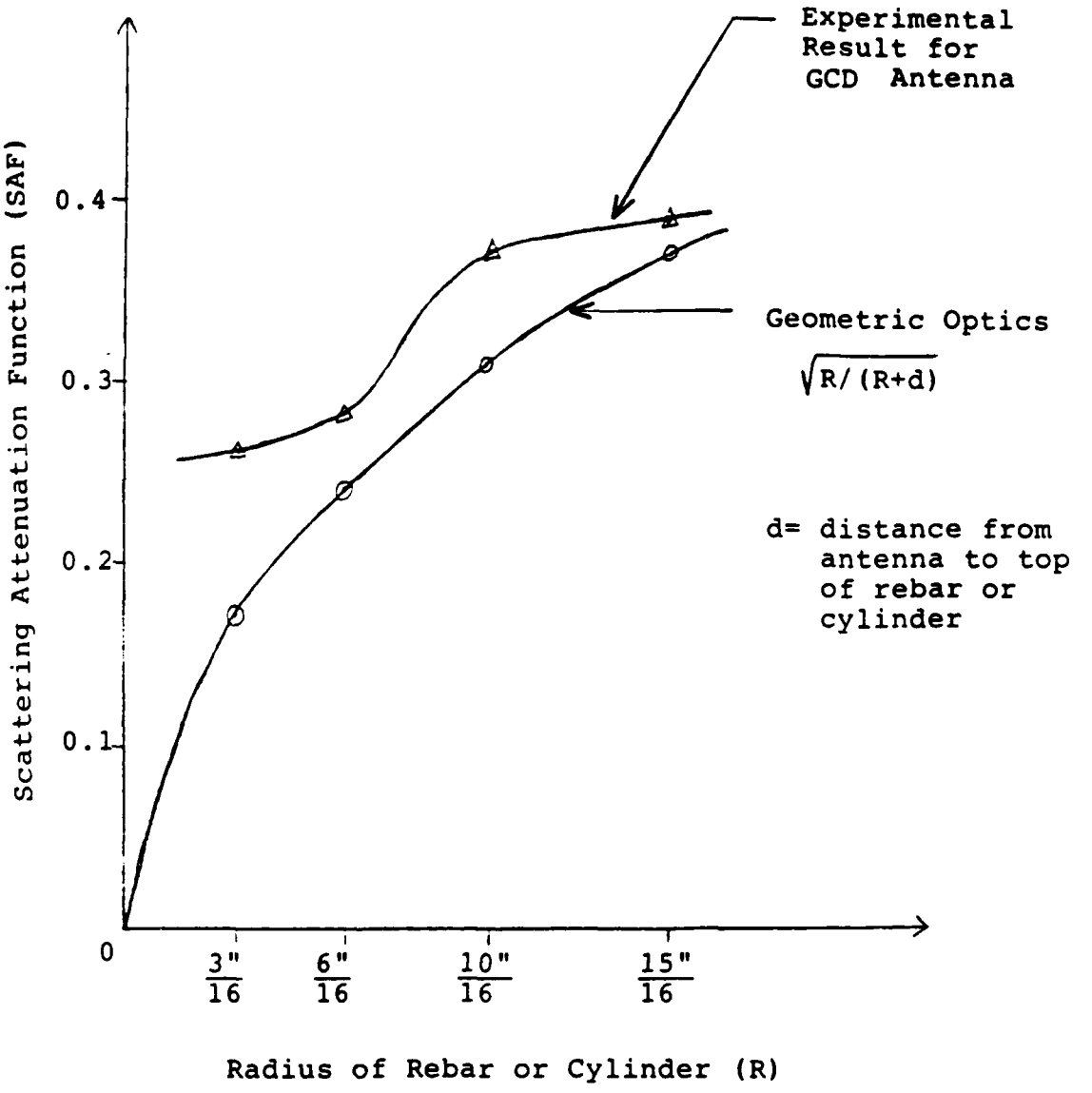

Figure 4

SCATTERING ATTENUATION FUNCTION (SAF) FOR GCD ANTENNA

(Rebar oriented parallel to polarization direction)

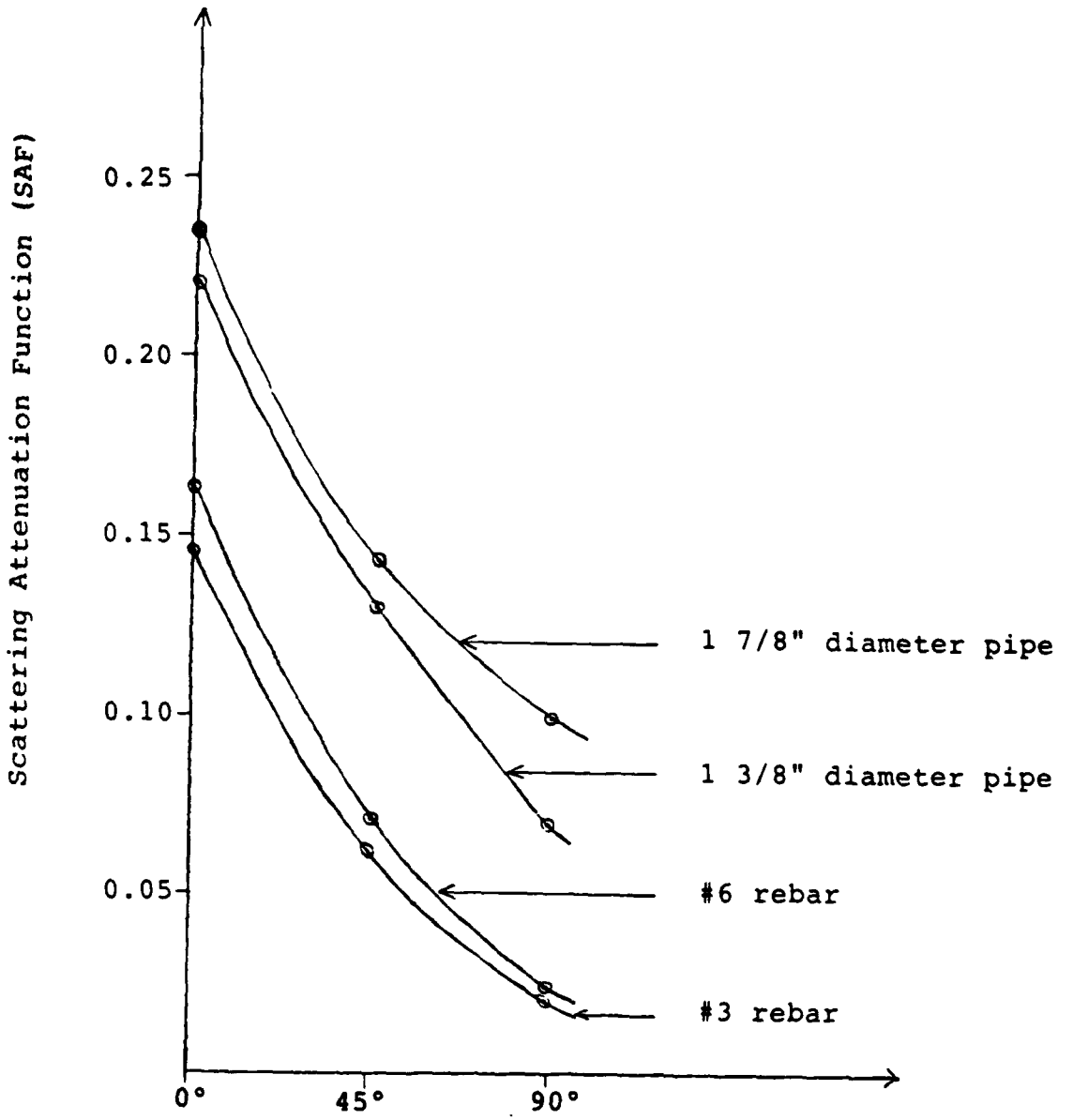

Figure 5

ORIENTATION EFFECT FOR AIR-COUPLED ANTENNA (ACH)

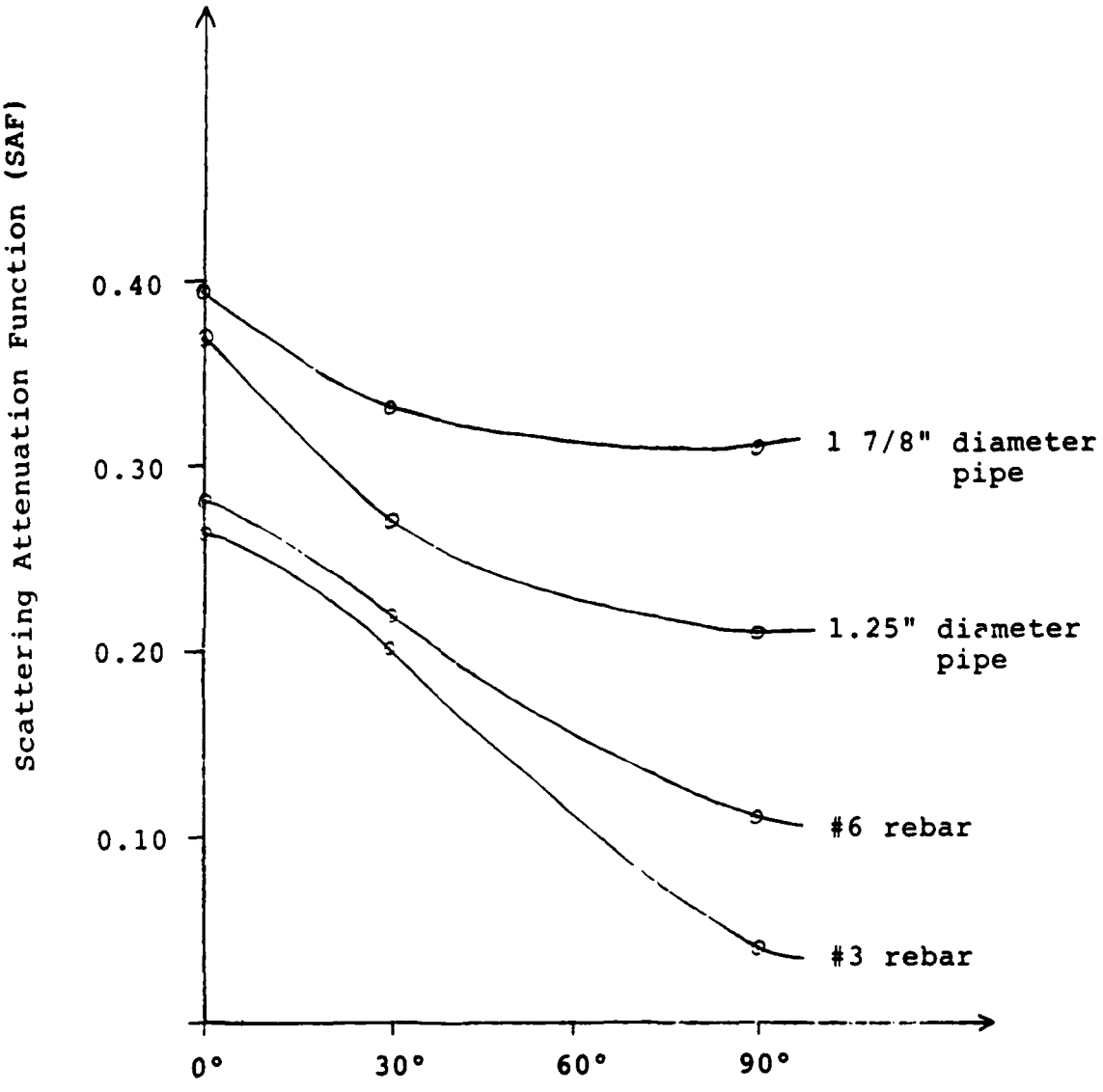

Figure 6

ORIENTATION EFFECT FOR GCD ANTENNA

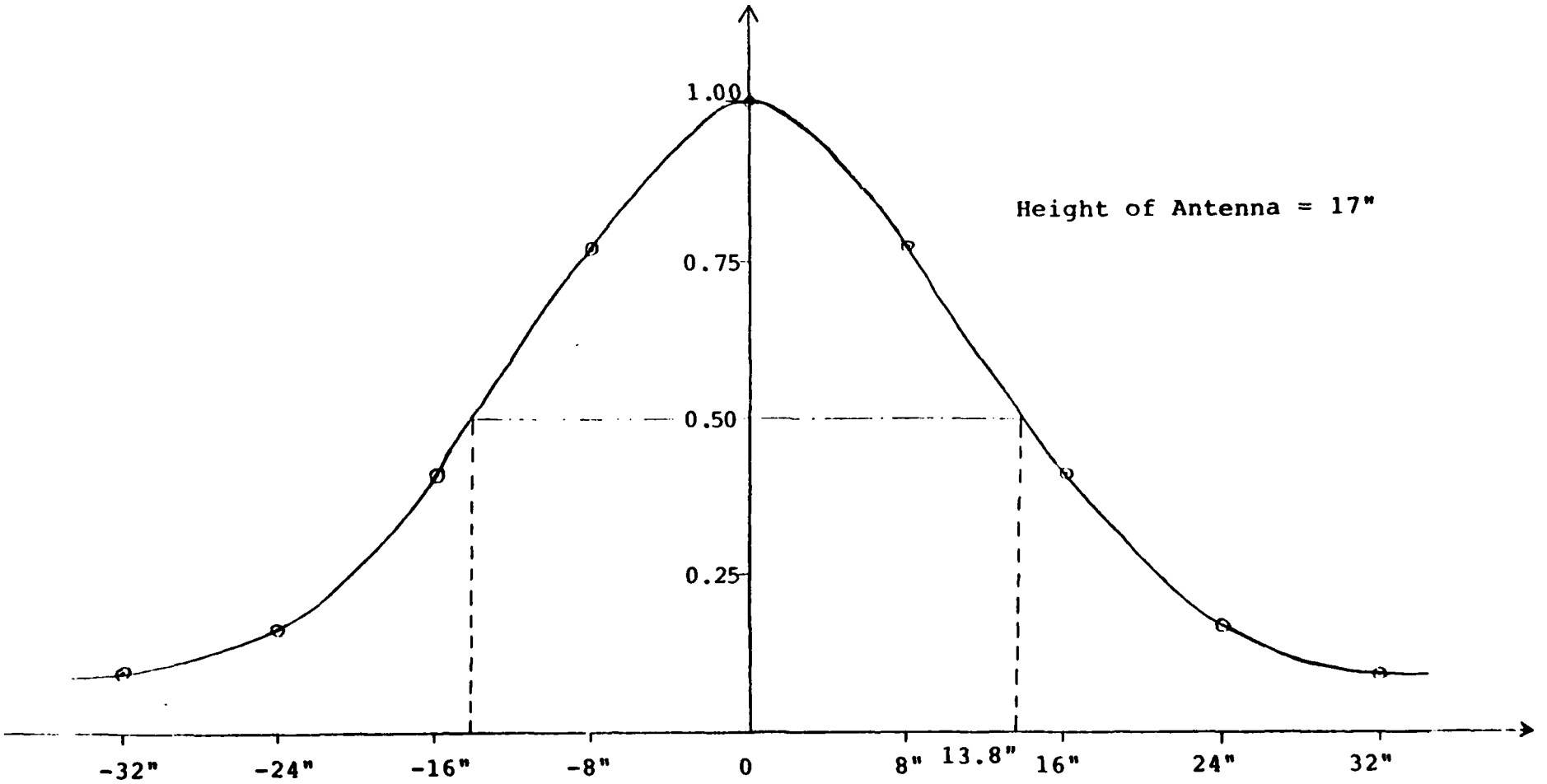

Figure 7

RADIATION PATTERN OF AIR-COUPLED ANTENNA IN A HORIZONTAL PLANE

(Rebar oriented parallel to polarization direction)

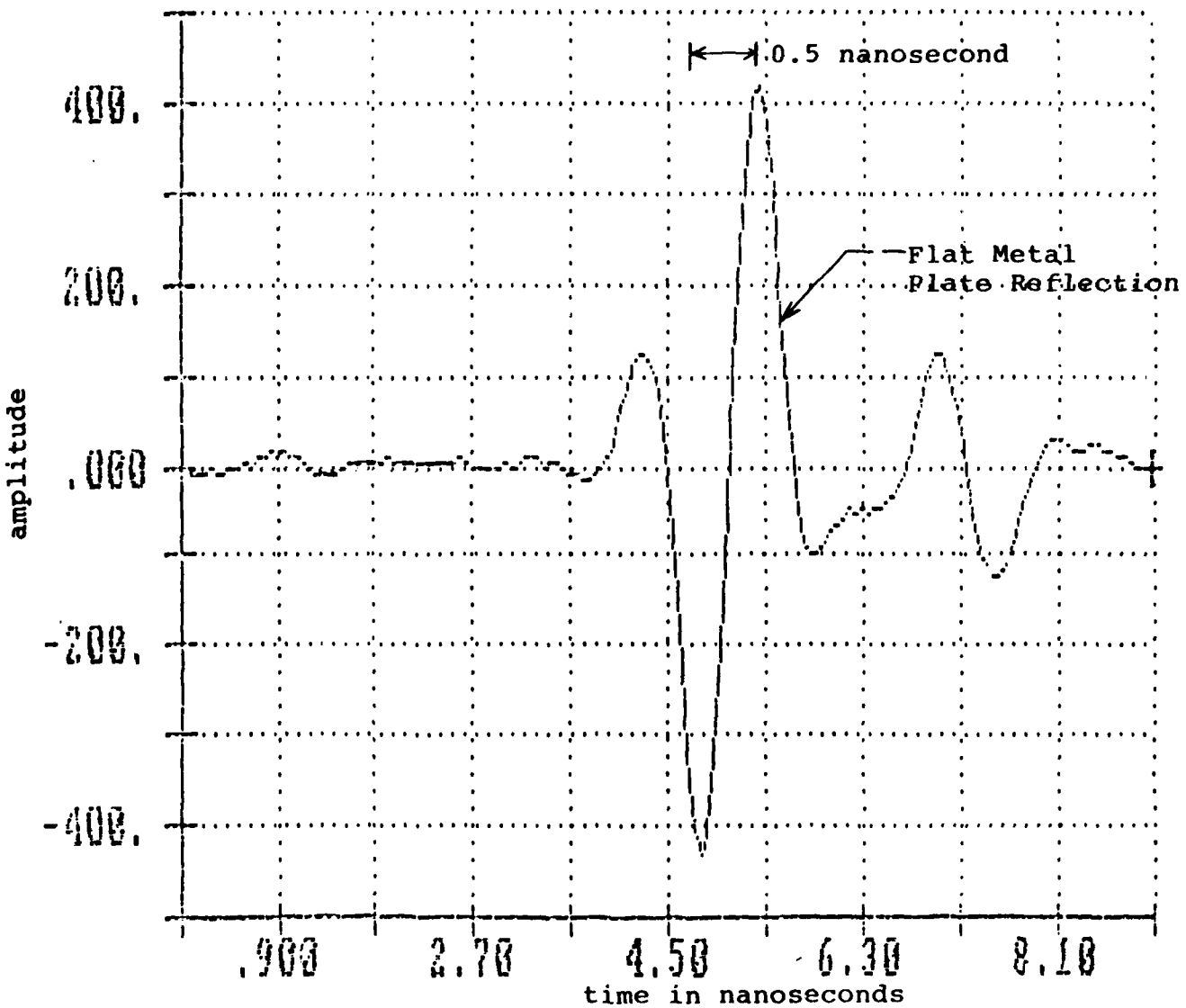

Figure 8

REFLECTION FROM FLAT METAL PLATE USING AIR-COUPLED ANTENNA

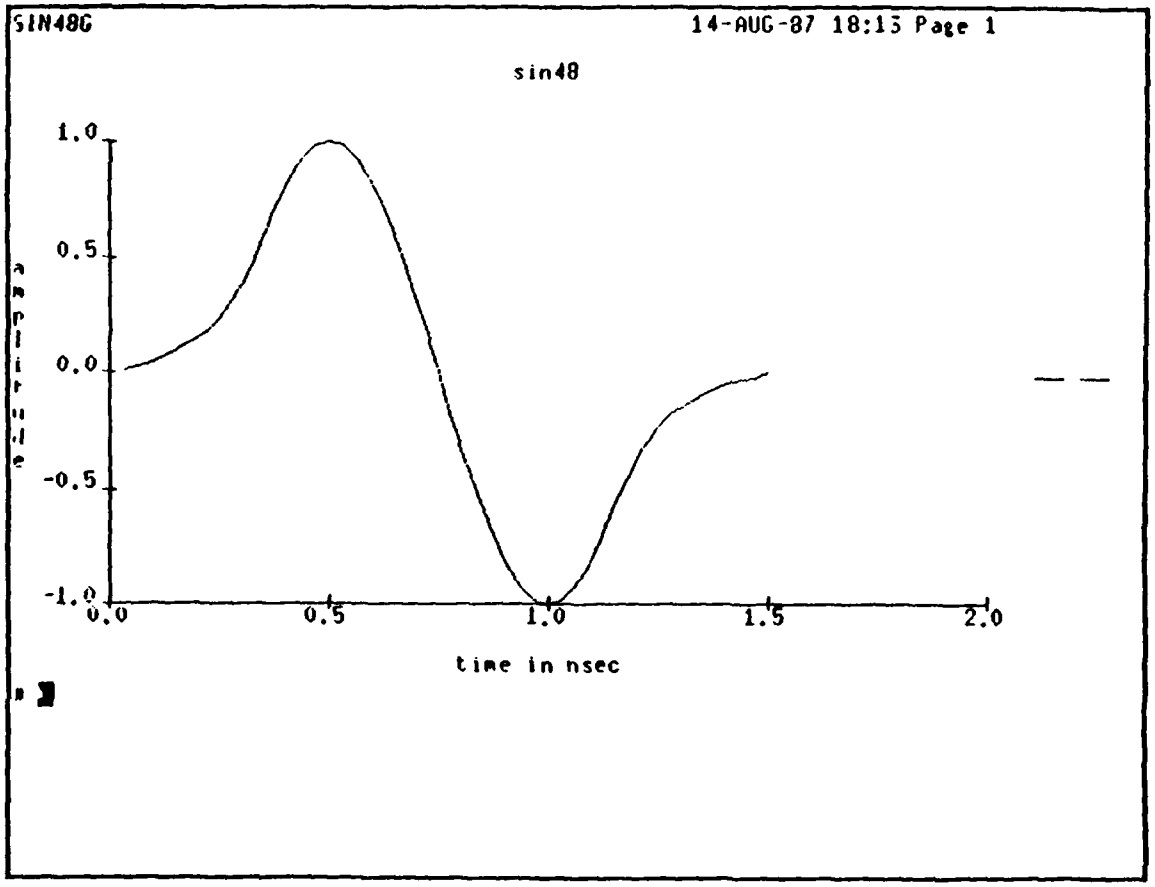

Figure 9

IDEALISED SINUSOIDAL TRANSMIT PULSE

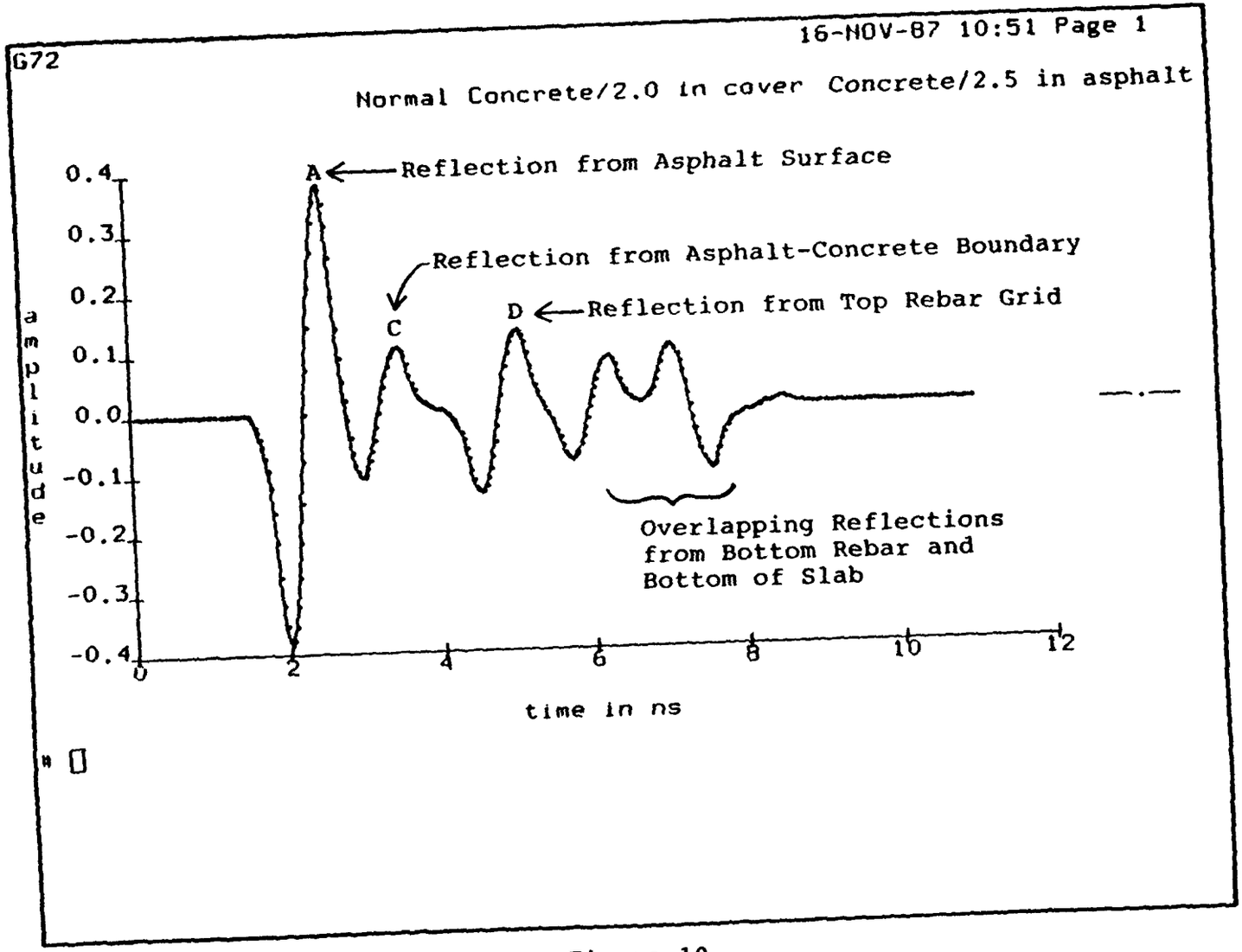

Figure 10

SYNTHESIZED WAVEFORM FOR NORMAL BRIDGE DECK

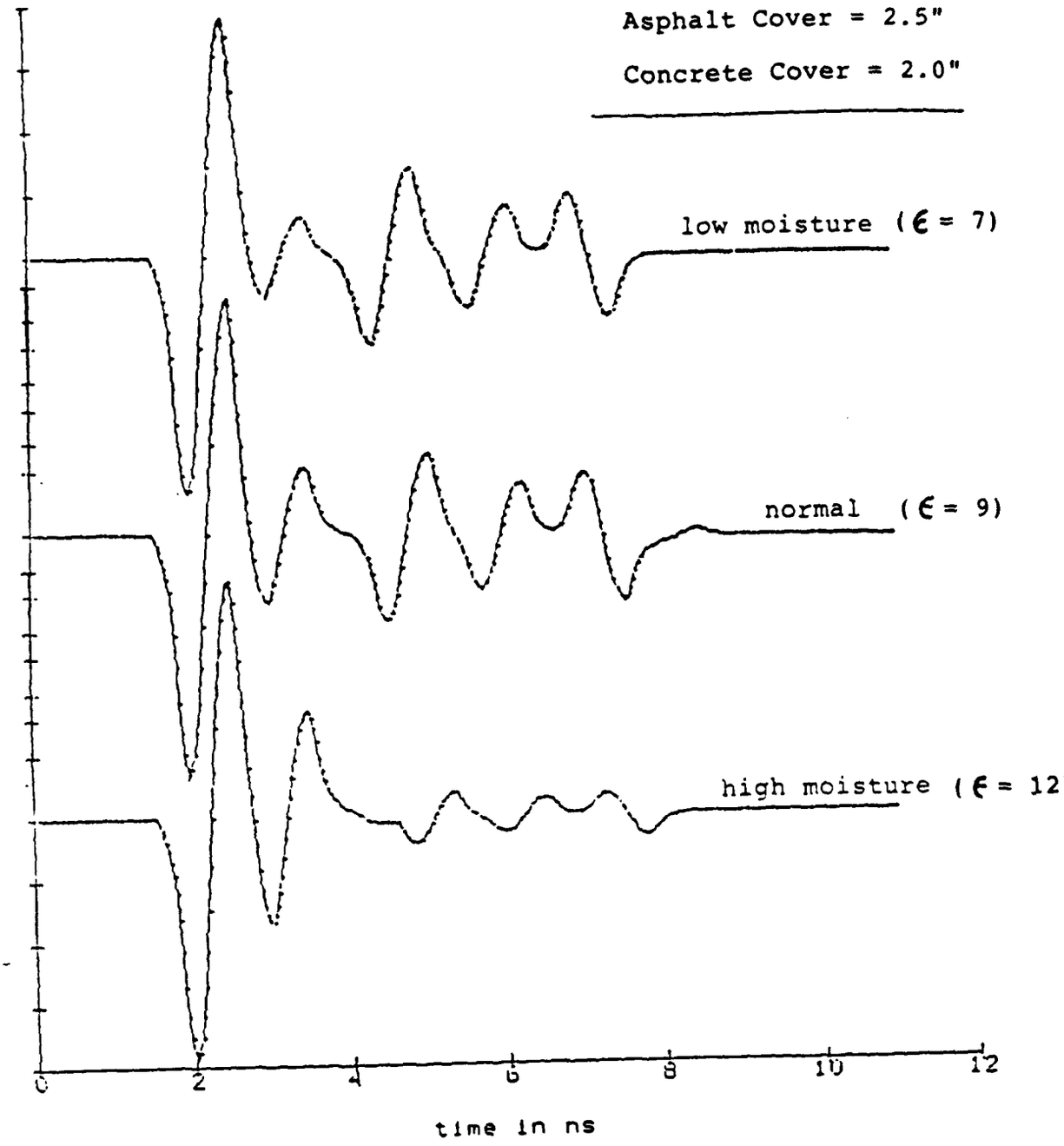

Figure 11

COMPUTED RADAR WAVEFORMS WITH VARYING MOISTURE CONTENT IN THE CONCRETE COVER

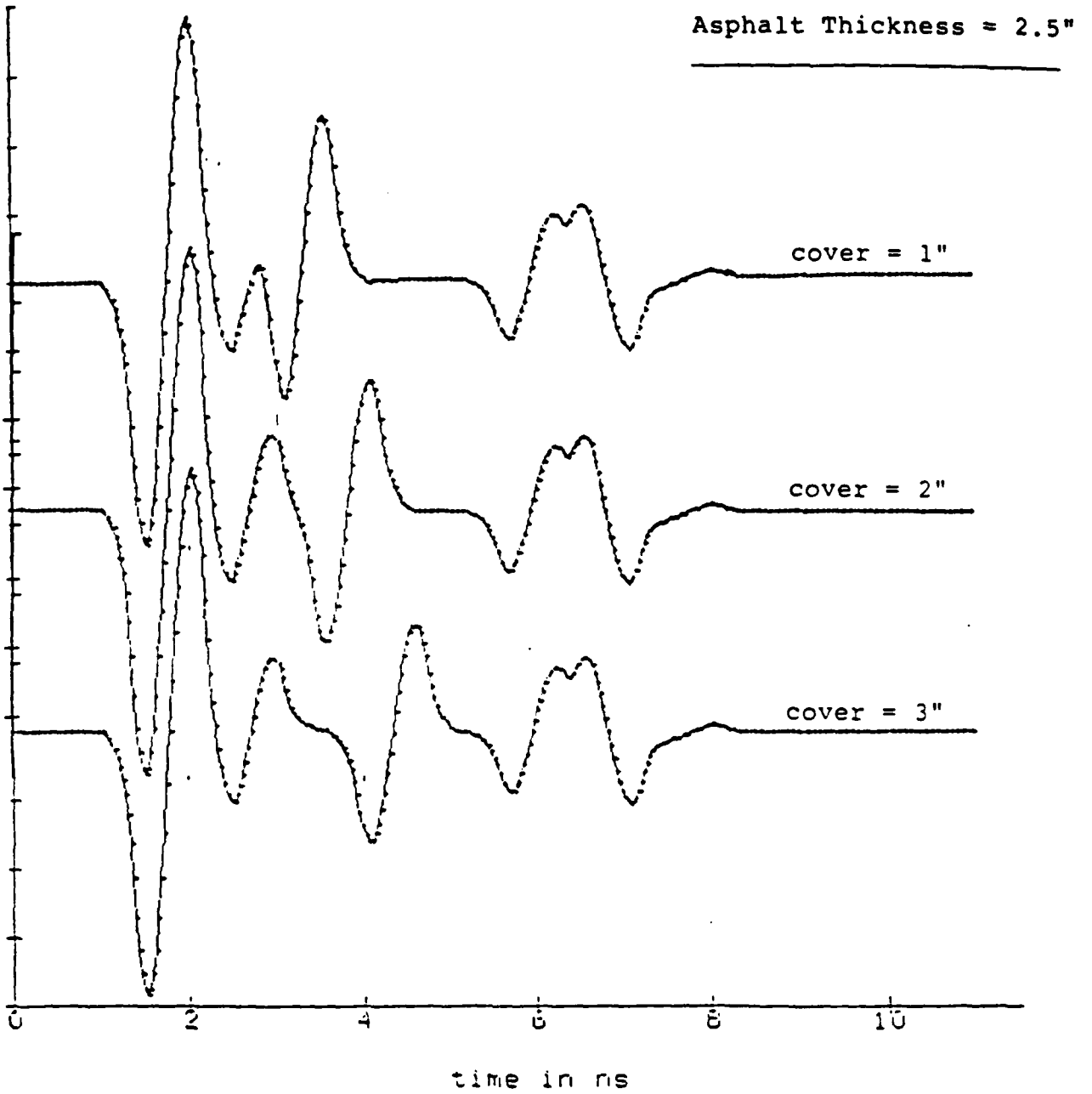

Figure 12

COMPUTED RADAR WAVEFORMS

WITH VARYING THICKNESS OF CONCRETE COVER

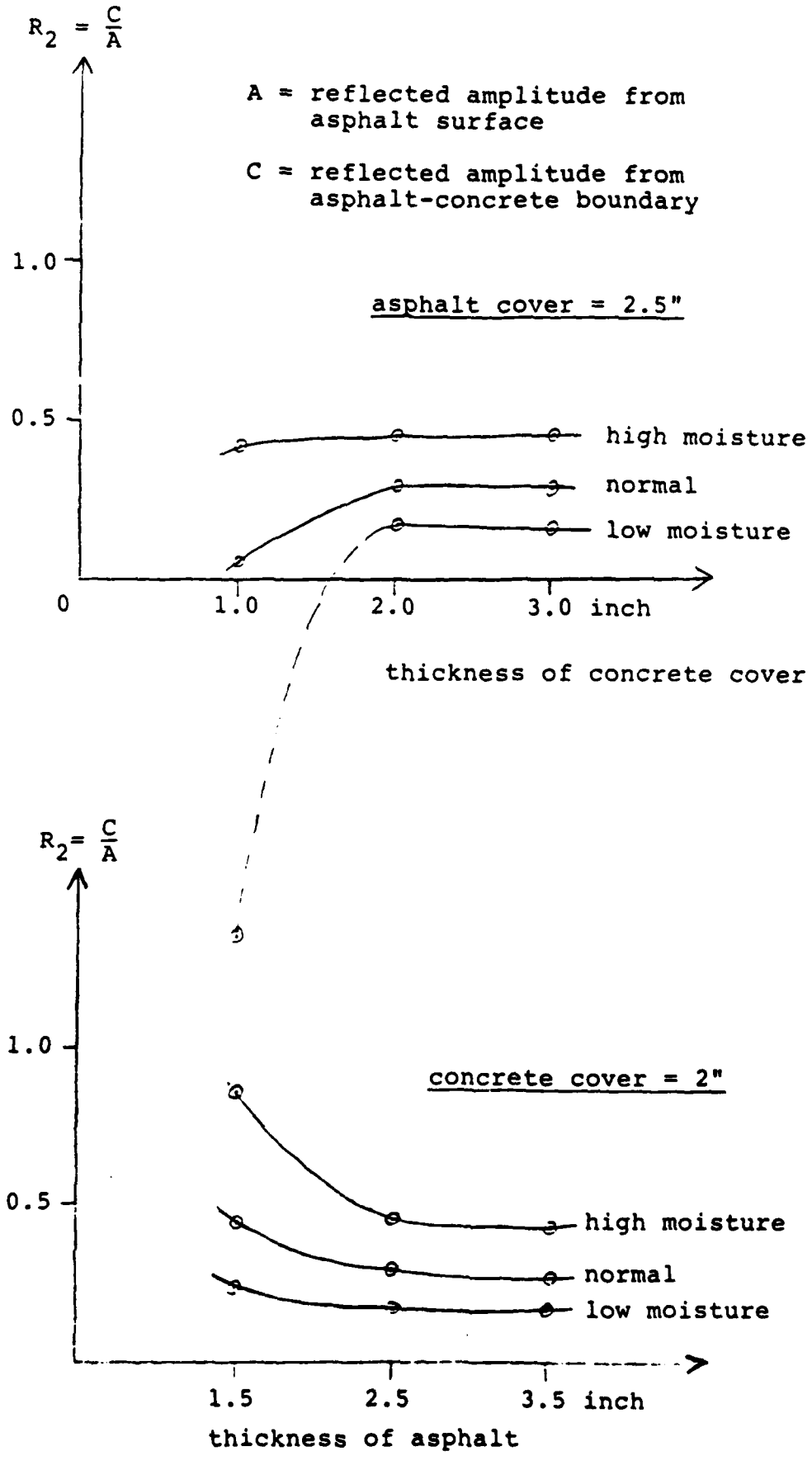

Figure 13 VARIATION OF R_2 WITH MOISTURE CONTENT

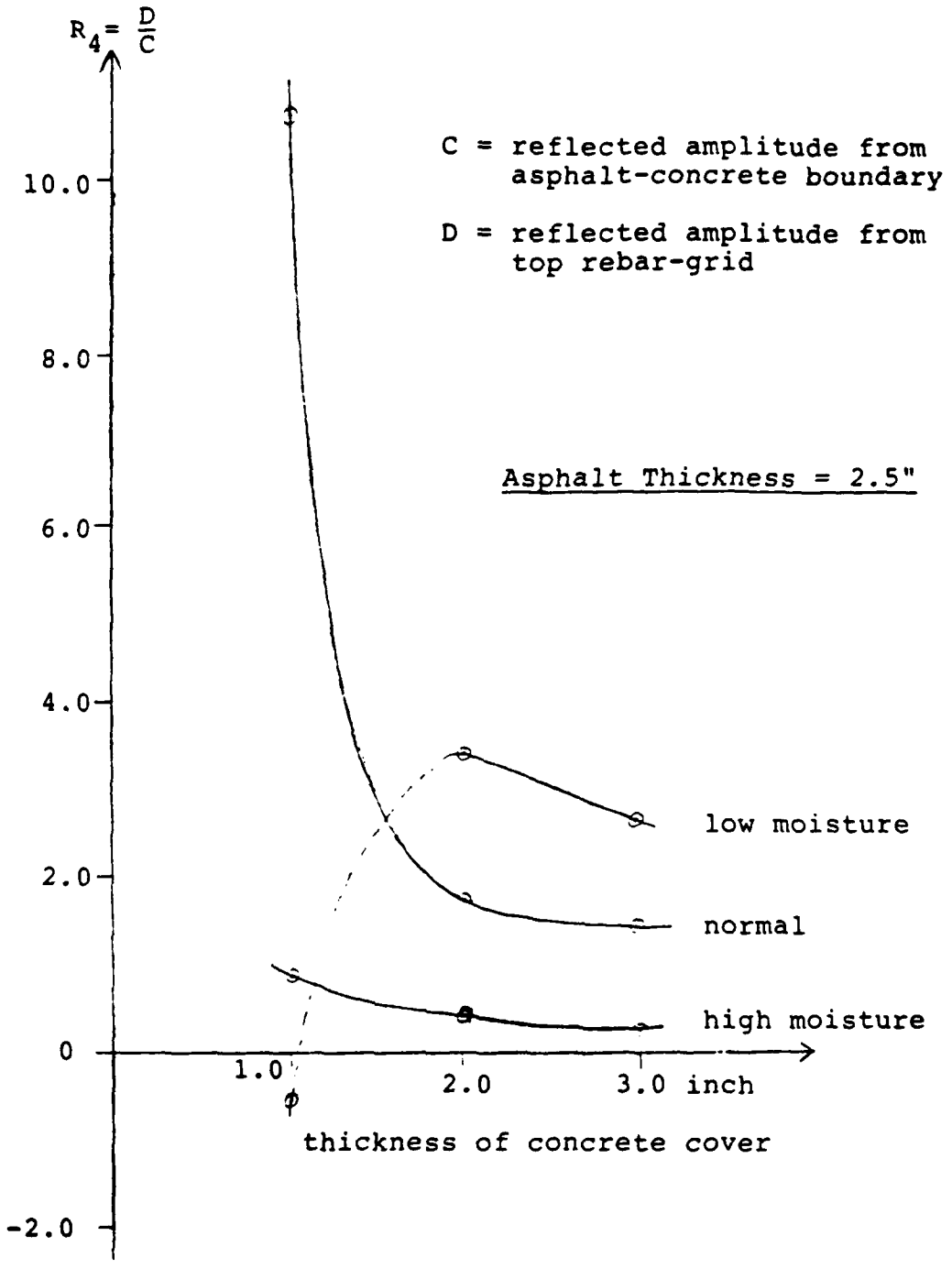

Figure 14

VARIATION OF R_4 WITH MOISTURE CONTENT

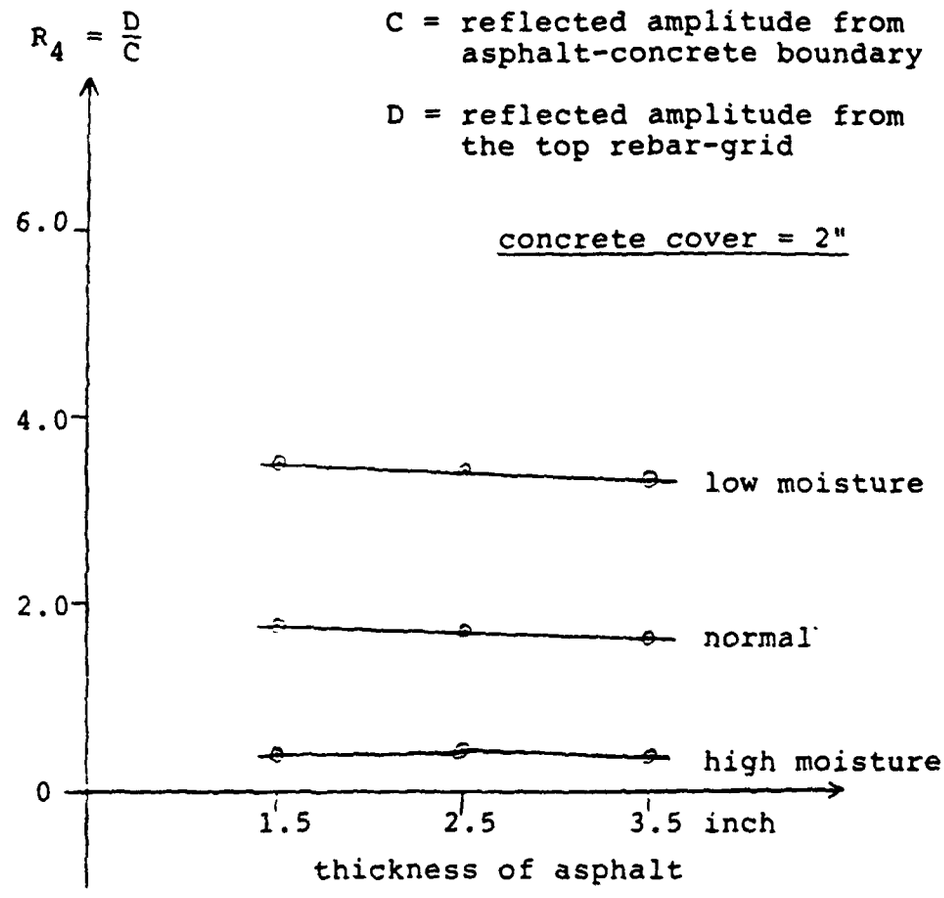

Figure 15

VARIATION OF R_4 WITH MOISTURE CONTENT

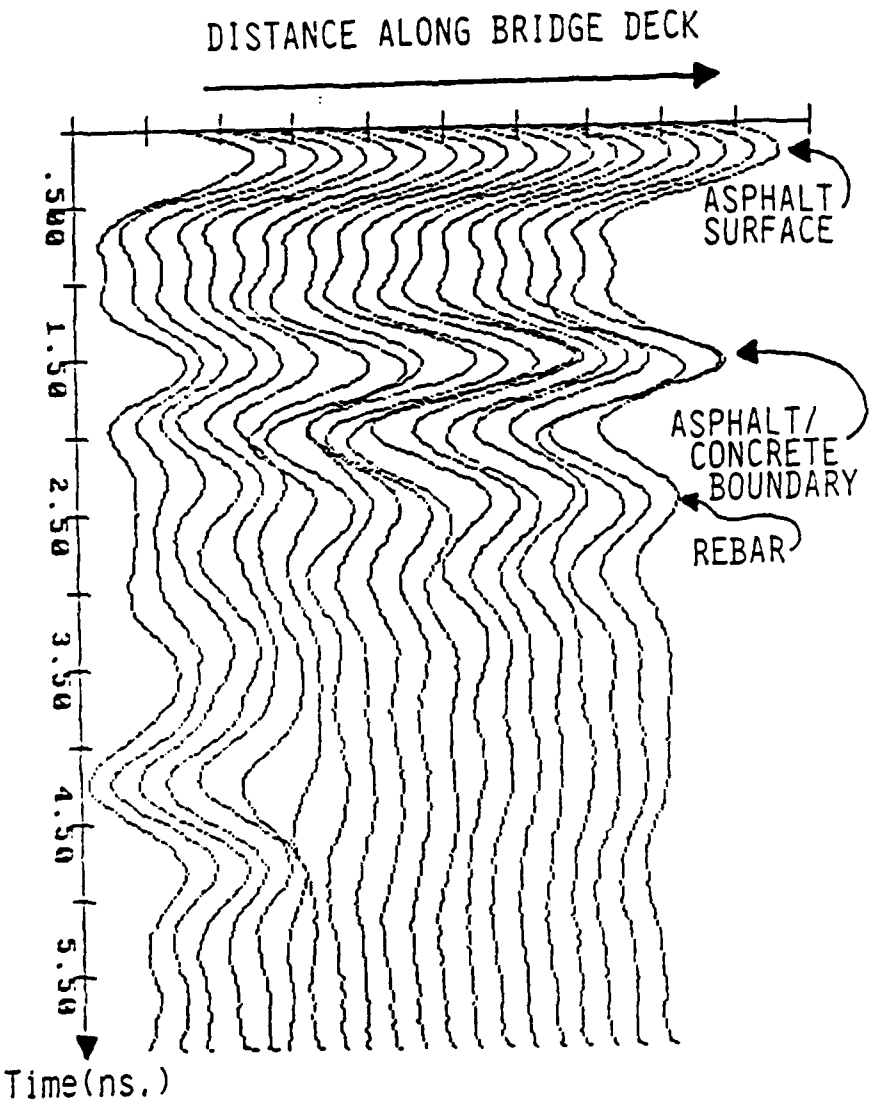

Figure 16

TYPICAL RADAR FIELD DATA

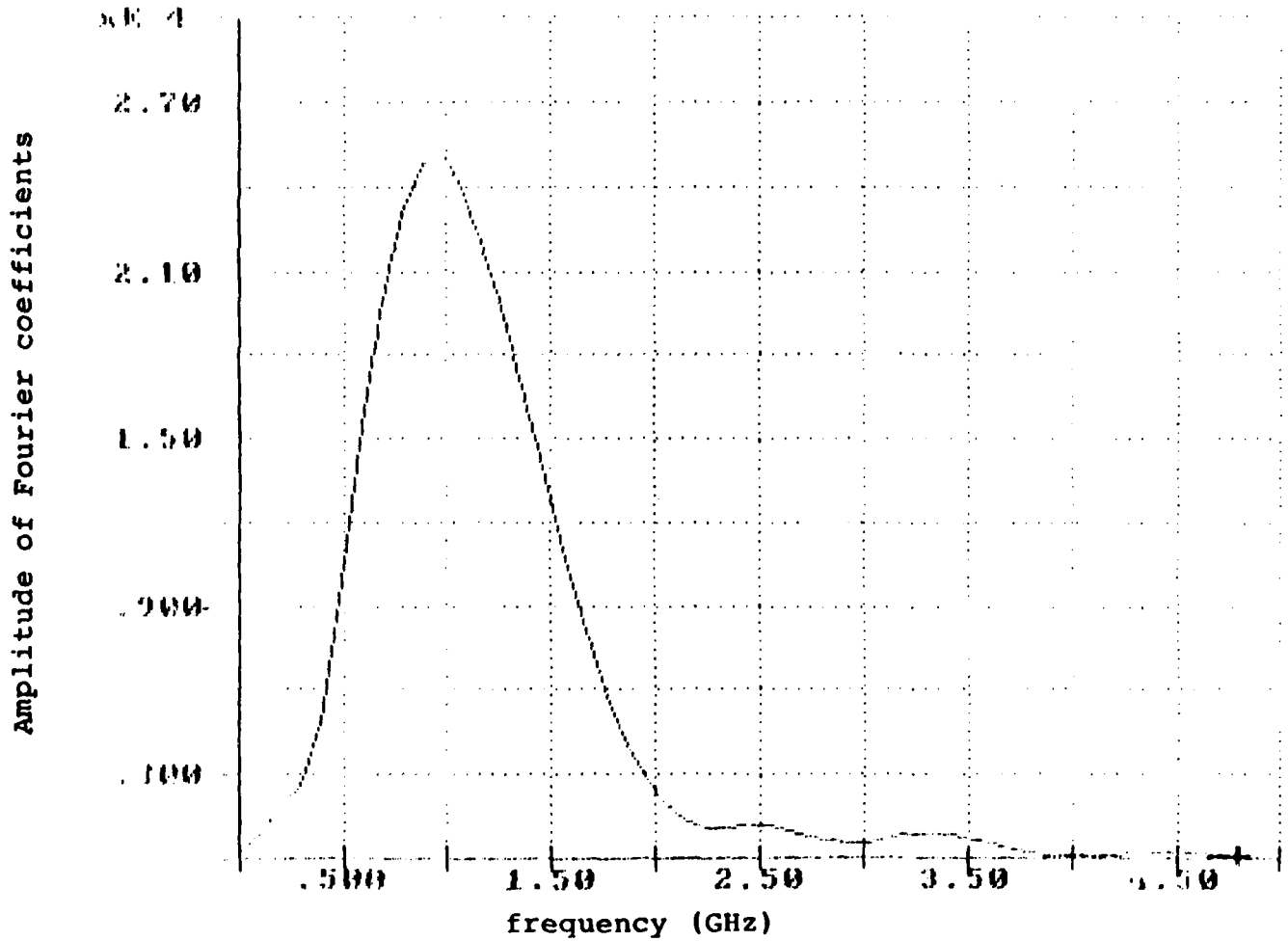

Figure 17

FOURIER TRANSFORM OF METAL PLATE REFLECTION FROM AIR-COUPLED ANTENNA

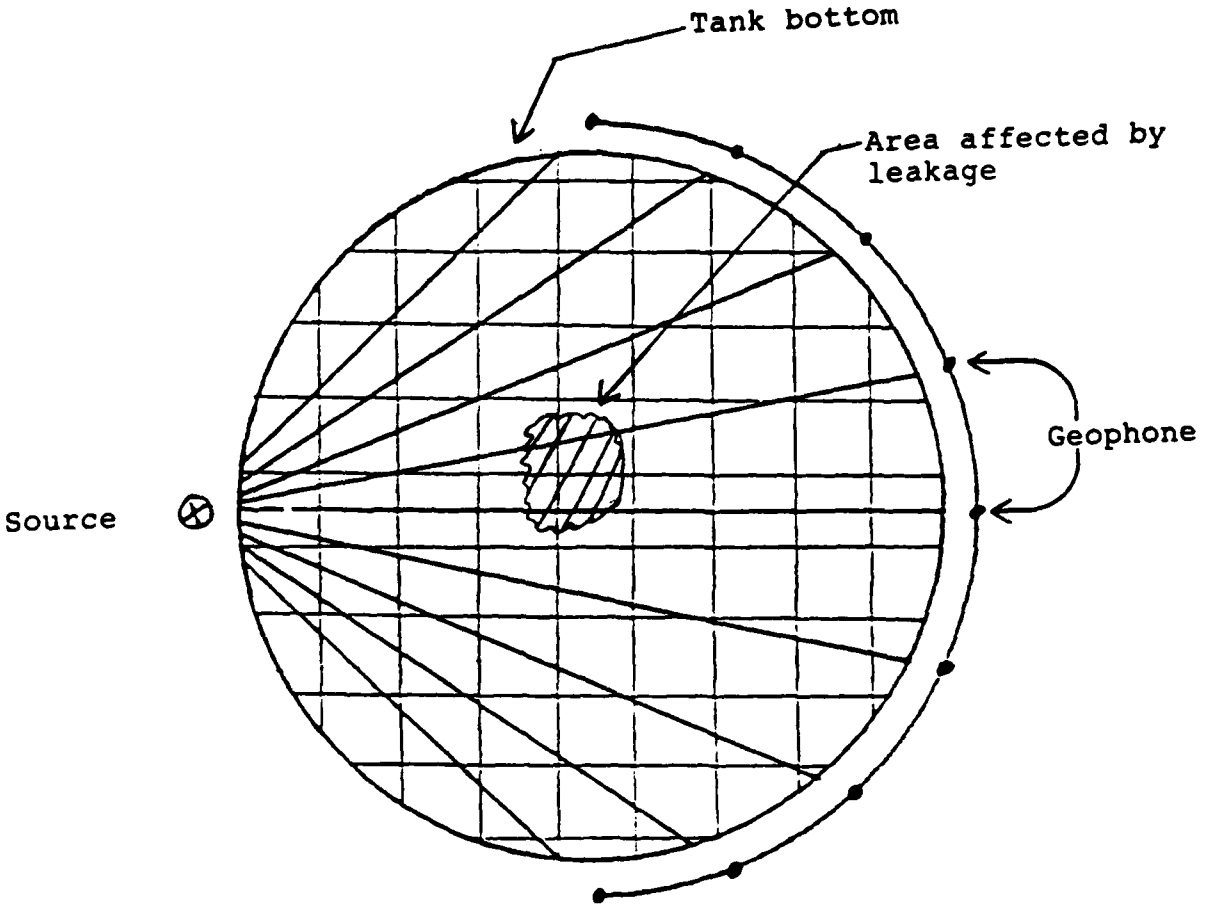

Plan View

Figure 18

SETUP FOR STONELEY WAVE MEASUREMENT IN FIELD